

## Multiple-scattering theory of magnetic x-ray circular dichroism

Christian Brouder and Muhammad Hikam

*Laboratoire de Physique du Solide, Université de Nancy I, Boîte Postale 239, F-54506 Vandoeuvre CEDEX, France*

(Received 1 May 1990; revised manuscript received 23 August 1990)

Multiple-scattering theory is generalized to take into account the effects of spin-orbit interaction and spin polarization of the photoelectron that are at the origin of the magnetic x-ray circular dichroism (MXD) effect observed in x-ray-absorption spectra where the final state of the photoelectron is delocalized. The basic framework of this treatment is nonrelativistic and relativistic corrections are considered as perturbations. The multiple-scattering approach sheds light on various aspects of MXD spectra: the relation between  $L_{II}$ - and  $L_{III}$ -edge magnetic signals, the difference between  $K$ -edge and  $L_{II,III}$ -edge spectra, and the analysis of spin-polarized extended x-ray-absorption fine structure. The equivalence between multiple-scattering and band-structure formalisms is used to show that useful information concerning the spin-polarized projected density of states of the photoabsorbing atom can be obtained from an analysis of MXD spectra.

### I. INTRODUCTION

The possibility of an interplay between magnetism and x-ray absorption was searched many times since Forman's experiments in 1914.<sup>1</sup> However, the first unambiguous evidence for this effect was observed only in 1986.<sup>2</sup> This discovery spurred the investigation of related phenomena, such as the magnetic Kerr effect<sup>3</sup> and Faraday rotation,<sup>4</sup> which were observed very recently. The sensitivity of x-ray absorption spectra to the magnetic state of the sample appears as a major new opportunity for x-ray-absorption spectroscopy and magnetism. Many applications of magnetic x-ray dichroism (MXD) have already been proposed (circular x-ray detectors and filters,<sup>5</sup> investigation of magnetism in transition metals,<sup>6-9</sup> rare earths<sup>10-12</sup> and alloys,<sup>2,7,10,12-15</sup> thin films,<sup>14</sup> multilayers,<sup>16</sup> etc.).

Since the early successful experiments, it was clear that the theoretical interpretation of MXD is much different when the magnetic orbitals probed by the x-ray-absorption process are localized or delocalized.

The case of localized orbitals such as  $M_{IV,V}$  edges of rare earths (probing  $4f$  states) or, to a lesser extent,  $L_{II,III}$  edges of light transition metals (probing  $3d$  states), was investigated with great success by the Dutch group.<sup>2,14,17,18</sup> The theoretical interpretation of the effect is now clear: MXD is due to the effect of selection rules governing transitions from the ground state to the multiplets obtained by coupling the ion state with the core hole and the localized photoelectron. If the influence of the crystal field is taken into account, the agreement between experiments and theory is very satisfactory.

The case of delocalized final states ( $L_{II,III}$  edges of rare earths and heavy transition metals,  $K$  edges of light transition metals) is not so clear. On the one hand, interpretation of experimental spectra in terms of spin-polarized density of states was proposed by the German group,<sup>6,7,10,11,13</sup> following the ideas put forward by Erskine and Stern.<sup>19</sup> It has a great heuristic value, and

was very useful to understand early experiments, but its validity is not clear. On the other hand, a fully relativistic theory of MXD was carried out by Strange and co-workers.<sup>20-25</sup> We should like to propose in this paper an alternative description of the MXD effect based on a nonrelativistic description of the electrons. We consider this treatment to be a viable alternative to that of Strange and collaborators for two reasons. Firstly, the nonrelativistic descriptions of magnetic materials and x-ray-absorption process are now well tested, and their range of validity is known. Secondly, nonrelativistic concepts are more familiar, and results given in terms of them are more intuitive. Our purpose is mainly to cast the heuristic approach in a rigorous framework, so that our conclusions can be used to understand experiments and envision new ones.

In this paper we use the spin-dependent local-density approximation and the multiple-scattering theory to investigate MXD at  $L_{II,III}$  edges, then at  $K$  edges. This part is valid over the whole energy range, down to the edge. Then we carry out a series expansion which leads us to a theory of spin-polarized x-ray-absorption fine structure (SPEXAFS). The case of  $K$ -edge spectra is more delicate since MXD observed is due to the action of spin-orbit coupling on the photoelectron states. Finally, we state our results in the band-structure language, so that experimental spectra can be analyzed in terms of spin density of states. The main physical results of this presentation are summarized in the conclusion.

This is a methodologic paper, its purpose is mainly to understand the physical principles underlying the MXD effect in delocalized orbitals. Therefore we treat the simplest (and most common) experimental situation where samples are powders. Moreover, since magnetic dipole transition probabilities are negligible in the x-ray range,<sup>26</sup> we consider only electric-dipole transitions. Sometimes, electric-quadrupole contributions can be large at the  $L_{II,III}$  edge of rare earths;<sup>27</sup> we shall not treat this additional complication here.

## II. BASIC NOTIONS AND NOTATION

First of all, the question we would like to address is that of the origin of MXD effects in delocalized orbitals. As was shown in a preliminary account of this theory,<sup>28</sup> it cannot be due to a direct polarization of the final-state space orbitals by the external field, because the order of magnitude of this effect is  $\mu_B B$  (where  $\mu_B$  is the Bohr magneton and  $B$  the applied field) which is typically  $10^{-4}$  eV and too small to be observed. By a time-symmetry argument it can be shown that, with spin-orbit coupling or spin polarization alone, MXD does not exist in the x-ray range (with delocalized final states).<sup>28</sup> Therefore, the MXD effect is due to an interplay of spin-orbit and exchange interactions, as emphasized in Refs. 14, 21, and 28.

Knowing that spin-orbit coupling and spin polarization are necessary for MXD, we immediately observe that there is a basic difference between x-ray-absorption spectra corresponding to core holes which are spherically symmetric ( $K, L_I$ ) or not (essentially  $L_{II}, L_{III}$ ).<sup>14,19</sup> In the latter case, spin-orbit coupling exists in the initial state, and MXD is directly sensitive to the spin polarization of the final state, via geometric factors (combinations of Clebsch-Gordan coefficients) that do not depend on energy. In the former case, spin-orbit coupling is absent in the initial state, and MXD effects are due to spin-orbit couplings in the final state, which are much weaker since the photoelectron is much less localized than the core hole (the order of magnitude of spin-orbit coupling is 100 eV for  $2p$  states of rare earths, and 0.05 eV for  $3d$  states of first row transition metals.<sup>29</sup> This is the basic reason why MXD effects are much weaker at  $K$  edges than at  $L_{II}, L_{III}$  edges. This is also why  $K$ -edge MXD is more difficult to interpret, as we shall see in Sec. IV. Since this is a first approach to MXD phenomena, we have neglected spin-orbit coupling in the final state for the calculation of MXD effects at  $L_{II,III}$  edges.

The basic concepts we shall use are as follows. We consider that a single electron description of the initial and final states is possible. The initial states are described by spin-orbitals  $|j, m_j\rangle$  where  $m_j$  varies from  $-j$  to  $j$  ( $j = \frac{1}{2}$  for an  $L_{II}$  edge,  $j = \frac{3}{2}$  for an  $L_{III}$  edge). When we do not consider the effect of spin orbit in the final state, the final states  $|f^\uparrow\rangle$  and  $|f^\downarrow\rangle$  are described, within the local-density approximation,<sup>30</sup> as eigenstates of the Hamiltonians

$$H^\uparrow = -\frac{\hbar^2}{2m}\Delta + V^\uparrow(\mathbf{r}), \quad (1)$$

$$H^\downarrow = -\frac{\hbar^2}{2m}\Delta + V^\downarrow(\mathbf{r}), \quad (2)$$

where  $V^\uparrow(\mathbf{r})$  and  $V^\downarrow(\mathbf{r})$  are energy-dependent potentials (we restrict the present treatment to real potentials, the generalization to complex potentials can be carried out along the line described in Ref. 31). Moreover, we con-

sider  $V^\uparrow(\mathbf{r})$  and  $V^\downarrow(\mathbf{r})$  as a sum of spherical nonoverlapping potentials embedded in a constant interstitial potential  $V_0^\uparrow$  and  $V_0^\downarrow$ . According to the spherical muffin-tin approximation, the potentials can be written

$$V^\uparrow(\mathbf{r}) = \frac{\hbar^2}{2m} \sum_i V_i^\uparrow(r_i), \quad (3)$$

$$V^\downarrow(\mathbf{r}) = \frac{\hbar^2}{2m} \sum_i V_i^\downarrow(r_i), \quad (4)$$

where  $V_i^s(r_i)$  is a spherical potential centered at nucleus  $i$  in the cluster, and  $r_i = |\mathbf{r} - \mathbf{R}_i|$ ,  $\mathbf{R}_i$  being the coordinate vector of site  $i$ . The factor  $\hbar^2/2m$  will simplify the following notation. From now on, the superscript  $s$  will stand for  $\uparrow$  or  $\downarrow$ , or for  $\frac{1}{2}$  or  $-\frac{1}{2}$ .

If we take the example of  $L_{II,III}$  edges, Eqs. (1) and (2) mean that we consider dipole transitions towards  $d_\uparrow$  and  $d_\downarrow$  final states, and not  $d_{3/2}$  and  $d_{5/2}$  final states. We made this choice because, since the crystal potential is not spherically symmetric,  $d_{3/2}$  and  $d_{5/2}$  are not eigenstates of the crystal, whereas up- and down-spin states are. Consequently, there is no transition from up- to down-spin states, and the Green function of the crystal is diagonal in spin coordinates (it can be considered as a Green function acting on up-spin states and a Green function acting on down-spin states).

Within the framework of multiple-scattering theory, we introduce two Green functions  $G^s(\mathbf{r}, \mathbf{r}')$  defined by

$$\left[ \kappa^s - \frac{2m}{\hbar^2} H^s \right] G^s(\mathbf{r}, \mathbf{r}') = \delta(\mathbf{r}, \mathbf{r}'), \quad (5)$$

where  $\kappa^s = (2m/\hbar^2)(E_i + \hbar\omega - V_0^s)$ . Because of exchange splitting,  $V_0^\uparrow \neq V_0^\downarrow$ , so that  $\kappa^\uparrow$  and  $\kappa^\downarrow$  are different for a given final-state energy  $E_f = E_i + \hbar\omega$ . We also introduce the scattering path operators defined by

$$\tau_{ij}^s = V_i^s \delta_{i,j} + V_i^s G^s V_j^s. \quad (6)$$

From this definition, scattering path operator  $\tau_{ij}^s$  is simply the  $t$  matrix of the whole system restricted to sites  $i$  and  $j$ . Physically,  $\tau_{ij}^s$  transforms an empty space wave function  $|\phi_0^s\rangle$  (for instance, a plane wave or a spherical wave) coming from site  $j$  into  $\tau_{ij}^s |\phi_0^s\rangle$ , which is the corresponding crystal wave function around site  $i$ .

The basic output of multiple-scattering calculations is the matrix elements of the scattering path operators:

$$\begin{aligned} \tau_{iLjL'}^s = \int d^3r_i \int d^3r'_j j_l(\kappa^s r_i) Y_L^*(\hat{\mathbf{r}}_i) \tau_{ij}^s(\mathbf{r}_i, \mathbf{r}'_j) \\ \times j_{l'}(\kappa^s r'_j) Y_{L'}(\hat{\mathbf{r}}'_j), \end{aligned} \quad (7)$$

where  $Y_L(\hat{\mathbf{r}}) = Y_L^m(\theta, \phi)$  for  $\hat{\mathbf{r}} = (\sin\theta \cos\phi, \sin\theta \sin\phi, \cos\theta)$  are spherical harmonics, the collective index  $L$  stands for  $(l, m)$ , and  $j_l$  are spherical Bessel functions. The importance of the scattering path operators stems from the fact that they can be used to write the Green function:<sup>32</sup>

$$G^s(\mathbf{r}_i, \mathbf{r}'_j) = \kappa^s \sum_{L, L'} R_{iL}^s(r_i) Y_L(\hat{\mathbf{r}}_i) \tau_{iLjL'}^s R_{jL'}^s(r'_j) Y_{L'}^*(\hat{\mathbf{r}}'_j) + \delta_{i,j} \kappa^s \sum_L R_{iL}^s(r_i) Y_L(\hat{\mathbf{r}}_i) J_{iL}^s(r_i) Y_L^*(\hat{\mathbf{r}}_i), \quad (8)$$

where  $R_{il}^s(r_i)$  and  $J_{il}^s(r_i)$  are two real solutions of the radial Schrödinger equation

$$\left[ \frac{d^2}{dr_i^2} + \frac{2}{r_i} \frac{d}{dr_i} + \kappa^s - \frac{l(l+1)}{r_i^2} - V_i^s(r_i) \right] \psi_l(r_i) = 0. \quad (9)$$

The former is regular at the origin and matches smoothly to  $j_l(\kappa^s r_i) \cot(\delta_{il}^s) - n_l(\kappa^s r_i)$  at the radius of the muffin-tin sphere  $i$ , the latter matches smoothly to  $j_l(\kappa^s r_i)$  at the muffin-tin radius.  $\delta_{il}^s$  is the  $l$ th phase shift for potential  $V_i^s(r_i)$ ,  $r_i^>$  ( $r_i^<$ ) is the larger (the smaller) of  $r_i, r_i'$ .

Using the scattering path operators and the Green functions, we shall investigate MXD in  $L_{II,III}$ -edge spectra of magnetic materials. The case of the  $K$  edge will require the spin-orbit coupling in the final state.

### III. MXD IN $L_{II,III}$ -EDGE SPECTRA

First, the general formulation of MXD spectra at the  $L_{II,III}$  edge of rare earths is given. Then we consider the case of the EXAFS region.

#### A. General formulation

The absorption cross section may be written as<sup>26</sup>

$$\sigma(\hat{\epsilon}, \omega) = 4\pi^2 \alpha \hbar \omega \sum_{f, m_j} |\langle f | \hat{\epsilon} \cdot \mathbf{r} | j m_j \rangle|^2 \delta(E_f - E_i - \hbar\omega), \quad (10)$$

where  $\hat{\epsilon}$  is the polarization vector of the x-ray beam.

As stated in Sec. II, in the case of  $L_{II,III}$  edges, the final states  $|f\rangle$  can be written as the product of a wave function  $f^s(\mathbf{r})$  by a spin state  $|s\rangle$ , and the absorption cross section is

$$\sigma(\hat{\epsilon}, \omega) = -4\pi\alpha\hbar\omega \left[ \frac{2m}{\hbar^2} \right] \sum_{m_j} \text{Im} [ \langle j m_j | (\hat{\epsilon} \cdot \mathbf{r})^* G^\uparrow(\mathbf{r}, \mathbf{r}') \hat{\epsilon} \cdot \mathbf{r}' | j m_j \rangle + \langle j m_j | (\hat{\epsilon} \cdot \mathbf{r})^* G^\downarrow(\mathbf{r}, \mathbf{r}') \hat{\epsilon} \cdot \mathbf{r}' | j m_j \rangle ]. \quad (13)$$

We assume also that the spin quantization axis is along the x-ray beam direction. This simplifies the calculation, and at the end of this section, we shall specify the changes that come when the two axes are not aligned. We use the optical definition of circular polarization.<sup>34</sup> Therefore a left- (right-) circular polarization corresponds to the photon helicity  $+\hbar$  ( $-\hbar$ ). The corresponding electric dipole interaction is

$$\hat{\epsilon}^\pm \cdot \mathbf{r} = \frac{1}{\sqrt{2}} (x \pm iy) = \mp \left[ \frac{4\pi}{3} \right]^{1/2} r Y_1^{\pm 1}(\hat{\mathbf{r}}) \quad (14)$$

for left and right polarization, respectively.

Introducing the expression of the Green function and of the initial states in the absorption cross section, and writing the integral of a product of three spherical harmonics in terms of Clebsch-Gordan coefficients [Eq. (3.192) of Ref. 35], we obtain the absorption coefficients for left- and right-circular polarization:

$$\sigma^\pm = -4\pi\alpha\hbar\omega \left[ \frac{2m}{\hbar^2} \right] \sum_{\Lambda, \Lambda', s} \kappa^s M_\Lambda^{s\pm} M_{\Lambda'}^{s\pm} \text{Im}(\tau_{0\Lambda 0\Lambda'}^s), \quad (15)$$

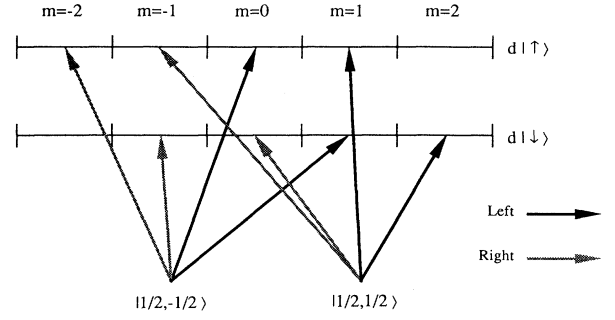


FIG. 1. Allowed transitions towards  $d$  states at an  $L_{II}$  edge (see text).

$$\sigma(\hat{\epsilon}, \omega) = 4\pi^2 \alpha \hbar \omega \sum_{f, m_j} ( |\langle f^\uparrow | \hat{\epsilon} \cdot \mathbf{r} | j m_j \rangle|^2 + |\langle f^\downarrow | \hat{\epsilon} \cdot \mathbf{r} | j m_j \rangle|^2 ) \delta(E_f - E_i - \hbar\omega). \quad (11)$$

The initial states can be written

$$|j m_j \rangle = \sum_{m, s} (l m \frac{1}{2} s | j m_j \rangle) \phi_{lj}(r) Y_l^m(\hat{\mathbf{r}}) |s\rangle, \quad (12)$$

where  $(l m \frac{1}{2} s | j m_j \rangle)$  is a Clebsch-Gordan coefficient and  $\phi_{lj}(r)$  is the radial part of the core hole state.  $\phi_{lj}(r)$  does not depend on spin, because  $H^\uparrow$  and  $H^\downarrow$  are almost identical near the nucleus.<sup>33</sup>

Writing the sum over final states in terms of the Green function, the absorption cross section becomes (with implicit summation over space variables and selection of spin  $|s\rangle$  in the initial state for  $G^s$ ).<sup>32</sup>

where 0 is the photoabsorbing site, and

$$M_\Lambda^{s\pm} = \mp \left[ \frac{2l+1}{2\lambda+1} \right]^{1/2} M_{\lambda lj}^s (l 0 1 0 | \lambda 0) \times \sum_m (l m \frac{1}{2} s | j m_j \rangle) (l m 1 \pm 1 | \lambda \mu), \quad (16)$$

with

$$M_{\lambda lj}^s = \int_0^\infty R_{0\lambda}^s(r) \phi_{lj}(r) r^3 dr. \quad (17)$$

To make the following calculation clearer, we start by considering the (model) case of the  $L_{II}$  edge of an isolated spin-polarized atom. The initial states are given by Eq. (12)

$$\begin{aligned} |\frac{1}{2}, -\frac{1}{2}\rangle &= \phi_{11/2}(r) [ (1/\sqrt{3}) Y_1^0(\hat{\mathbf{r}}) |\downarrow\rangle \\ &\quad - (\sqrt{2/3}) Y_1^{-1}(\hat{\mathbf{r}}) |\uparrow\rangle ], \\ |\frac{1}{2}, \frac{1}{2}\rangle &= \phi_{11/2}(r) [ -(1/\sqrt{3}) Y_1^0(\hat{\mathbf{r}}) |\uparrow\rangle \\ &\quad + (\sqrt{2/3}) Y_1^1(\hat{\mathbf{r}}) |\downarrow\rangle ]. \end{aligned} \quad (18)$$

The  $d$  orbitals are split by exchange (we neglect transitions towards  $s$  states) and the transition rules for left (right)-circular polarization are  $m_f = m_i + 1$  ( $m_f = m_i - 1$ ), where  $m_i$  is the magnetic quantum number of the spherical harmonics in the initial state. The allowed transitions are shown in Fig. 1. Using Eq. (16) we have the following partial transition probabilities for left-circular polarization:

$$\begin{aligned} m_j = -\frac{1}{2} &\rightarrow (m_f = 1, m_s = -\frac{1}{2}): \frac{3}{5}\sigma^\downarrow, \\ m_j = -\frac{1}{2} &\rightarrow (m_f = 0, m_s = +\frac{1}{2}): \frac{2}{5}\sigma^\uparrow, \\ m_j = +\frac{1}{2} &\rightarrow (m_f = 1, m_s = +\frac{1}{2}): \frac{3}{5}\sigma^\uparrow, \\ m_j = +\frac{1}{2} &\rightarrow (m_f = 2, m_s = -\frac{1}{2}): \frac{12}{5}\sigma^\downarrow, \end{aligned} \quad (19)$$

where  $\sigma^\uparrow$  ( $\sigma^\downarrow$ ) are reduced transition probabilities proportional to the square of  $M_{211/2}^\uparrow$  ( $M_{211/2}^\downarrow$ ). Therefore we see that the main contribution to the absorption cross section is the transition from  $m_j = +\frac{1}{2}$  to the  $d$  state with  $m_f = 2$  and down spin. Because of this term, left-circular x rays make preferential transitions towards down-spin states. Summing over initial and final states, we obtain the absorption cross section:

$$\sigma^+ = \sigma^\uparrow + 3\sigma^\downarrow. \quad (20)$$

Conversely, right-circular x rays make preferential transi-

tions towards up-spin states and we have

$$\sigma^- = 3\sigma^\uparrow + \sigma^\downarrow. \quad (21)$$

This preference of circularly polarized x rays for transitions towards definite spin states is the essence of the magnetic x-ray circular dichroism.

After this treatment of a simple atomic model, we shall see that analogous results are obtained for the general case of a powdered sample. It is shown in Ref. 36 that the scattering path operator matrix elements can be expanded as a sum of  $(c, \gamma)$ -spherical tensors

$$\tau_{0\lambda 0\lambda'}^s = \sum_{c, \gamma} \tau_{00}^s(\lambda, \lambda'; c, \gamma) (-1)^{\lambda-\mu} (\lambda \mu \lambda' \mu' | c \gamma). \quad (22)$$

The terms  $\tau_{00}^s(\lambda, \lambda'; c, \gamma)$  contain the same information as the original scattering path operators; they can be used to obtain all the one-body physical quantities concerning the central site 0. They have the properties of transforming under rotation as spherical harmonics and are very useful for investigating powders since, in that case, all the terms  $\tau_{00}^s(\lambda, \lambda'; c, \gamma)$  are canceled by the spherical average, except for the isotropic component  $\tau_{00}^s(\lambda, \lambda; 0, 0)$ :<sup>36</sup>

$$\langle \tau_{0\lambda 0\lambda'}^s \rangle = \frac{\tau_{00}^s(\lambda, \lambda; 0, 0)}{\sqrt{2\lambda+1}} \delta_{\lambda, \lambda'} \quad (23)$$

and the absorption cross section for powders can be written

$$\sigma^\pm = -4\pi\alpha\hbar\omega \left[ \frac{2m}{\hbar^2} \right] \sum_{\lambda s} \kappa^{s2} \frac{2l+1}{(2\lambda+1)^{3/2}} (M_{\lambda l j}^s)^2 (I010|\lambda 0)^2 \text{Im}[\tau_{00}^s(\lambda, \lambda; 0, 0)] \sum_m (lm \frac{1}{2} s | jm + s)^2 (lm \pm 1 | \lambda m \pm 1)^2. \quad (24)$$

The sum of products of Clebsch-Gordan coefficients have been evaluated for an  $L_{II}$  edge ( $l=1, j=\frac{1}{2}$ ), and for an  $L_{III}$  edge ( $l=1, j=\frac{3}{2}$ ). The results can be written conveniently as follows. For an  $L_{II}$  edge,

$$\sigma_{L_{II}}^+ = \sigma_{21/2}^\uparrow + 3\sigma_{21/2}^\downarrow + 2\sigma_{01/2}^\uparrow, \quad (25)$$

$$\sigma_{L_{II}}^- = 3\sigma_{21/2}^\uparrow + \sigma_{21/2}^\downarrow + 2\sigma_{01/2}^\downarrow. \quad (26)$$

For an  $L_{III}$  edge,

$$\sigma_{L_{III}}^+ = 5\sigma_{23/2}^\uparrow + 3\sigma_{23/2}^\downarrow + \sigma_{03/2}^\uparrow + 3\sigma_{03/2}^\downarrow, \quad (27)$$

$$\sigma_{L_{III}}^- = 3\sigma_{23/2}^\uparrow + 5\sigma_{23/2}^\downarrow + 3\sigma_{03/2}^\uparrow + \sigma_{03/2}^\downarrow, \quad (28)$$

where

$$\begin{aligned} \sigma_{ij}^s &= -4\pi\alpha\hbar\omega \left[ \frac{2m}{\hbar^2} \right] \frac{1}{9\sqrt{2l+1}} (\kappa^s M_{l1j}^s)^2 \\ &\times \text{Im}[\tau_{00}^s(l, l; 0, 0)]. \end{aligned} \quad (29)$$

## B. Discussion

The physical meaning of the above coefficients is, for instance, that  $\sigma_{2j}^\uparrow$  represents a transition probability towards  $d$  final states ( $\lambda=2$ ) with spin up (i.e., spins oriented parallel to the x-ray beam direction). Since the spin polarization of  $s$  states can be neglected when compared with that of  $d$  states, Eq. (25) shows that, at an  $L_{II}$  edge,

left-polarized x rays make preferential transitions towards down spins. The reverse is true at an  $L_{III}$  edge. The coefficients that rule the spin preference are purely geometrical. They are a consequence of angular momentum coupling and do not depend on energy. Therefore, MXD experiments carried out at  $L_{II,III}$  edges give an unambiguous identification of the spin polarization of the  $d$  final states (or more precisely of the  $d$  projection of the final states). Equations (25)–(28) have been obtained by Erskine and Stern<sup>19</sup> for the case of fcc nickel. Our results are more general, since they are valid for any crystallographic structure, provided the sample is a powder. Additional terms would be present in Eqs. (25)–(28) for non-cubic single crystals.

The present results can easily be compared with experiment. It was shown by Schütz *et al.* that, in many cases, the quantity  $(\sigma^+ - \sigma^-)/(\sigma^+ + \sigma^-)$  is approximately twice as large at the  $L_{II}$  edge as at the  $L_{III}$  edge and that the sign of the effect is reversed. We can assume, as is usual, that the transitions towards  $s$  states are small.<sup>37</sup> Then, if  $\sigma_{23/2}^s \approx \sigma_{21/2}^s$  (which corresponds to the fact that the radial wave functions of the  $j=\frac{1}{2}$  and  $\frac{3}{2}$  core holes are not very different), we have, at an  $L_{II}$  edge,  $\sigma^+ + \sigma^- = 4\sigma^\uparrow + 4\sigma^\downarrow$ ,  $\sigma^+ - \sigma^- = -2\sigma^\uparrow + 2\sigma^\downarrow$ . At an  $L_{III}$  edge,  $\sigma^+ + \sigma^- = 8\sigma^\uparrow + 8\sigma^\downarrow$ ,  $\sigma^+ - \sigma^- = 2\sigma^\uparrow - 2\sigma^\downarrow$ . Therefore we see that the magnetic effects  $\sigma^+ - \sigma^-$  are reversed at the  $L_{II}$  and  $L_{III}$  edges, and that

$$\left[ \frac{\sigma^+ - \sigma^-}{\sigma^+ + \sigma^-} \right]_{L_{II}} \simeq -2 \left[ \frac{\sigma^+ - \sigma^-}{\sigma^+ + \sigma^-} \right]_{L_{III}} . \quad (30)$$

Notice that, since  $\sigma_{2j}^{\uparrow}$  is dominant, the MXD effect at  $L_{II,III}$  edges probes the spin polarization of the  $d$  final states of the photoabsorbing atom. This is an attractive feature of MXD in x-ray-absorption spectra: the spin polarization is probed selectively for each value of  $l$ .

Another important point is the understanding of what happens when the x-ray polarization is fixed, and the direction of the applied magnetic field is reversed. It can be shown by a time-symmetry argument that the MXD effect observed when reversing the external field is identical with the effect obtained by reversing the circular polarization or the spin-quantization axis. In other words,  $\sigma^{\uparrow}(-\mathbf{B}) = \sigma^{\downarrow}(\mathbf{B})$  and  $\sigma^{\downarrow}(-\mathbf{B}) = \sigma^{\uparrow}(\mathbf{B})$ , where  $\mathbf{B}$  is the external field. Therefore the spin orientation of the final states relative to the external field direction can be deduced from the sign of  $\sigma^{\uparrow}(\mathbf{B}) - \sigma^{\downarrow}(\mathbf{B})$  obtained from experimental spectra. This conclusion is very important in practice, since MXD spectra give the spin orientation of the  $d$  electrons of the photoabsorbing species. For instance, assume that you send left-circular x-rays on a magnetic sample in an external magnetic field. Let  $\sigma^{\uparrow}(\mathbf{B})$  [ $\sigma^{\downarrow}(-\mathbf{B})$ ] be the spectrum observed when the external magnetic field is parallel (antiparallel) to the x-ray beam direction. At an  $L_{II}$  edge we have

$$\begin{aligned} \Delta\sigma &= \sigma^{\uparrow}(\mathbf{B}) - \sigma^{\downarrow}(-\mathbf{B}) \\ &= \sigma^{\uparrow}(\mathbf{B}) - \sigma^{\downarrow}(\mathbf{B}) \\ &= 2(\sigma^{\downarrow} - \sigma^{\uparrow}) . \end{aligned} \quad (31)$$

If, experimentally,  $\Delta\sigma > 0$ , we have  $\sigma^{\downarrow} > \sigma^{\uparrow}$  and, from the band-structure interpretation discussed in Sec. V, this means that we have more down-spin final states, in other words the photoelectron spin is polarized preferentially antiparallel to the applied field. Neglecting the effect of the core hole, we can conclude that if  $\Delta\sigma > 0$  for a certain energy range above the edge, the density of down spins is larger than the density of up spins for the same energy range above the Fermi energy.

We would like to complete this section by describing how the results are modified when the final-state spin direction is not aligned with the x-ray beam. This can occur either in helimagnetic or not saturated samples, or by not aligning the external field along the x-ray beam.

If the x-ray wave-vector coordinates are  $(k \sin\theta \cos\phi, k \sin\theta \sin\phi, k \cos\theta)$  in a reference frame where the  $z$  axis is along the spin-quantization axis, then the electric-dipole matrix for left-circular polarization is obtained by rotating  $\hat{\mathbf{e}}^+$ . This gives us

$$\hat{\mathbf{e}} \cdot \mathbf{r} = - \left[ \frac{4\pi}{3} \right]^{1/2} r \sum_p D_{p1}^1(\phi, \theta, 0) Y_1^p(\hat{\mathbf{r}}) , \quad (32)$$

where  $D_{p1}^1(\phi, \theta, 0)$  is a Wigner rotation matrix parametrized by the Euler angles  $\phi$ ,  $\theta$ , and 0. Then the previous calculation can be repeated, and we obtain for an  $L_{II}$  edge

$$\begin{aligned} \sigma_{L_{II}}(\theta) &= (2 - \cos\theta)\sigma_{21/2}^{\uparrow} + (2 + \cos\theta)\sigma_{21/2}^{\downarrow} \\ &\quad + (1 + \cos\theta)\sigma_{01/2}^{\uparrow} + (1 - \cos\theta)\sigma_{01/2}^{\downarrow} \end{aligned} \quad (33)$$

and for an  $L_{III}$  edge

$$\begin{aligned} \sigma_{L_{III}}(\theta) &= (4 + \cos\theta)\sigma_{23/2}^{\uparrow} + (4 - \cos\theta)\sigma_{23/2}^{\downarrow} \\ &\quad + (2 - \cos\theta)\sigma_{03/2}^{\uparrow} + (2 + \cos\theta)\sigma_{03/2}^{\downarrow} , \end{aligned} \quad (34)$$

where  $\theta$  is the angle between the spin-up direction and the x-ray wave vector, for left-circular polarization.

If the incident x-ray beam is not fully circularly polarized, its state of polarization can be described by  $P$ , the degree of polarization [ $P=0$  for purely natural (unpolarized) light,  $P=1$  for fully (elliptically) polarized light], and by  $\chi$  which describes polarization ellipticity. These Poincaré parameters are described in Ref. 34. To take account of this general polarization state, we can use the coherency matrix of the beam<sup>34</sup> to show that the factor  $\cos\theta$  should be replaced by the factor  $-P \cos\theta \sin 2\chi$  in Eqs. (33) and (34). This gives us the  $L_{II,III}$  absorption coefficient of an x-ray beam with the most general polarization state by a magnetic material where the spins have any orientation. If the spins of the final states of the absorbing species have not always the same orientation, as in helimagnetic materials, a proper average must be carried out over  $\theta$ .<sup>2</sup>

### C. SPEXAFS at $L_{II,III}$ edges

The presence of a spin-polarized extended x-ray-absorption fine structure (SPEXAFS) in the magnetic x-ray dichroism spectra was observed first at the  $L_{II,III}$  edges of gadolinium in  $\text{Gd}_3\text{Fe}_5\text{O}_{12}$ .<sup>12</sup> This effect was confirmed at the  $L_{II,III}$  edges of cerium in  $\text{CeFe}_2$ .<sup>15</sup> At the  $K$  edge of transition metals the fine structure is much weaker.

In this section, we show how the standard expansion of scattering path operators in multiple-scattering series can lead us to an understanding of the fine structure observed experimentally. From this study, it will be possible to state which characteristics of the system can be drawn from an analysis of the fine structure of magnetic x-ray dichroism.

Formula (29) gives effective transition probabilities towards up and down spins. They are essentially the product of an atomic factor  $(\kappa^s M_{ij}^s)^2$ , which varies smoothly without oscillation, by the imaginary part of a scattering path operator  $\tau_{00}^s(l, l; 0, 0)$  which represents the influence of the whole crystal. In SPEXAFS, as in standard EXAFS, this latter term is the origin of the fine structure. EXAFS oscillations are due to photoelectron backscattering by neighboring atoms. We obtain them by expanding the scattering path operator in a multiple-scattering series up to second order (single scattering). It is shown in Ref. 36 that, to second order, the multiple-scattering series is

$$\tau_{00}^s(l, l; 0, 0) = - \frac{\sqrt{2l+1}}{\kappa^s} t_{0l}^s + \tau_{00}^{s(2)}(l, l; 0, 0) + \dots , \quad (35)$$

where the second term is the usual EXAFS contribution due to single scattering by neighboring atoms:

$$\tau_{00}^{s(2)}(l, l; 0, 0) = \frac{\sqrt{2l+1}}{\kappa^s} (t_{0l}^s)^2 \sum_{j, l'} (2l'+1) t_{jl'}^s \sum_a (l0l'0|a0)^2 [h_a^+(\kappa^s R_{0j})]^2, \quad (36)$$

with  $t_{jl'}^s = \sin \delta_{jl'}^s \exp i \delta_{jl'}^s$ .  $h_a^+$  is a spherical Hankel function and  $R_{0j}$  is the distance from the photoabsorbing site to site  $j$ .

Since, at this stage, we do not need the accuracy of spherical wave EXAFS formulas, we shall use the plane-wave EXAFS approximation obtained by taking the asymptotic limit of spherical Hankel functions.<sup>38</sup> This yields

$$\sigma_{ij}^s = 4\pi\alpha\hbar\omega \left[ \frac{2m}{\hbar^2} \right] \frac{1}{9} \kappa^s (M_{l1j}^s)^2 \sin^2(\delta_{0l}^s) \left[ 1 + (-1)^l \sum_j \frac{1}{(\kappa^s R_{0j})^2} \text{Im} \left[ \exp[2i(\kappa^s R_{0j} + \delta_{0l}^s)] \sum_{l'} (-1)^{l'} (2l'+1) t_{jl'}^s \right] \right]. \quad (37)$$

As expected, Eq. (37) would be identical to the standard EXAFS formula if there were no spin polarization. It is possible to test experimentally the validity of this expression. Measuring the  $L_{II}$  and  $L_{III}$  edges of an element, we can obtain  $\sigma_{21/2}^s$  and  $\sigma_{23/2}^s$  from Eqs. (25)–(28). Then, the ratio  $\sigma_{21/2}^s/\sigma_{23/2}^s$  should be structureless.

We assume, as usually, that the “atomic” contribution has been removed by the normalization procedure (which can be quite delicate in practice), and that we work on the quantities

$$\chi_l^s = 1 + (-1)^l \sum_j \frac{1}{(\kappa^s R_{0j})^2} \text{Im} \left[ \exp[2i(\kappa^s R_{0j} + \delta_{0l}^s)] \sum_{l'} (-1)^{l'} (2l'+1) t_{jl'}^s \right]. \quad (38)$$

Since the effect of spin polarization is small, we can write

$$\kappa^s = \kappa + s \Delta\kappa, \quad \delta_{jl}^s = \delta_{jl} + s \Delta\delta_{jl}. \quad (39)$$

This gives us the SPEXAFS formula:

$$\chi_l^M = \chi_l^\uparrow - \chi_l^\downarrow \quad (40)$$

$$\begin{aligned} &= (-1)^l \sum_{j, l'} (-2\Delta\kappa/\kappa + \Delta\delta_{jl'} \cot \delta_{jl'}) \frac{(-1)^{l'} (2l'+1) \sin(\delta_{jl'})}{(\kappa R_{0j})^2} \sin(2\kappa R_{0j} + 2\delta_{0l} + \delta_{jl'}) \\ &+ (-1)^l \sum_{j, l'} (2\Delta\kappa R_{0j} + 2\Delta\delta_{0l} + \Delta\delta_{jl'}) \frac{(-1)^{l'} (2l'+1) \sin(\delta_{jl'})}{(\kappa R_{0j})^2} \cos(2\kappa R_{0j} + 2\delta_{0l} + \delta_{jl'}). \end{aligned} \quad (41)$$

This SPEXAFS formula has an interesting structure. The first line of Eq. (41) contains terms that are in phase with the EXAFS signal. Its first term is small at EXAFS energies since  $2\Delta\kappa/\kappa = \Delta E/E$  and  $\Delta E \simeq 0.1$  eV,<sup>39</sup> its second line depends on the spin-polarization of the back-scattering atoms. The second line of Eq. (41) contains terms that are in quadrature with the EXAFS signal. For the case studied in Ref. 12, SPEXAFS signal seems to be mainly in quadrature with the EXAFS signal, so that this latter term is dominant. Schütz *et al.* state that SPEXAFS probes the local magnetic environment of the absorbing atom.<sup>12</sup> This is supported by our present results. A part of the SPEXAFS signal depends on the spin polar-

ization of the neighbors, which is zero for nonmagnetic species. Moreover, in the case of  $\text{Gd}_3\text{Fe}_5\text{O}_{12}$  studied in Ref. 12, the  $d$  orbitals of iron are strongly polarized, and their contribution to SPEXAFS oscillations is noticeable. However, another part of SPEXAFS oscillations depends on the neighbor distances and on the spin polarization of the absorbing species. This part contains contribution from all the neighbors, so that the SPEXAFS signal is due, not only to the magnetic neighbors, but also to the spin polarization of the absorbing species.

Notice that Eq. (41) can also be written in a somewhat more familiar form

$$\begin{aligned} \chi_l^M &= (-1)^l (-2\Delta\kappa/\kappa) \sum_j \frac{A_j}{\kappa R_{0j}^2} \sin(2\kappa R_{0j} + 2\delta_{0l} + \phi_j) + (-1)^l (2\Delta\kappa R_{0j} + 2\Delta\delta_{0l}) \sum_j \frac{A_j}{\kappa R_{0j}^2} \cos(2\kappa R_{0j} + 2\delta_{0l} + \phi_j) \\ &+ (-1)^l \sum_{j, l'} \Delta\delta_{jl'} \frac{(-1)^{l'} (2l'+1)}{(\kappa R_{0j})^2} \sin(2\kappa R_{0j} + 2\delta_{0l} + 2\delta_{jl'}), \end{aligned} \quad (42)$$

where  $A_j$  and  $\phi_j$  are the standard amplitude and phase factors of the  $j$ th neighbor used in the EXAFS formula and defined as<sup>37</sup>

$$A_j \exp(i\phi_j) = \sum_{l'} \frac{(-1)^{l'} (2l'+1)}{\kappa} \sin(\delta_{jl'}) \exp(i\delta_{jl'}). \quad (43)$$

Notice that, since the factor  $\Delta\delta_{jl'}$  in the last term of Eq. (42) is due to the spin polarization of the phase shift of the  $j$ th neighbor, SPEXAFS can be observed also when the absorbing atom is not spin polarized,<sup>40</sup> or more precisely when the photoabsorber atomic potentials for up and down spins are equal.

#### IV. MXD IN $K$ -EDGE SPECTRA

If, for a  $K$  edge we carry out the same calculation as in Sec. III, we find that the absorption by left-circularly polarized x rays is not different from that by right-circularly polarized x rays. Therefore, as explained in Sec. II, MXD at the  $K$  edge is due to spin-orbit coupling in the final state. In magnetic materials, the spin-orbit coupling is the origin of magnetic anisotropy and is treated as a perturbation of the pure spin states. This is valid here since spin-orbit coupling is much weaker than magnetic band splitting<sup>29,41,42</sup> and experimental resolution of x-ray-absorption spectroscopy. Moreover, this retains the familiar language of spin-polarized electron states.

##### A. Perturbation of wave functions by spin-orbit coupling

Let  $\psi^s$  be the unperturbed magnetic states. The spin-orbit coupling is written  $\sum_i \xi_i(r_i) l_i \cdot \sigma_i$ , where  $\xi_i(r_i)$  is the spin-orbit operator at site  $i$ ,  $l_i = (l_i^x, l_i^y, l_i^z)$  is the local angular momentum (divided by  $\hbar$ ), and  $\sigma_i = (\sigma^x, \sigma^y, \sigma^z)$  are Pauli matrices. Since the spin-orbit term is a function of the derivative of the potential, it is spherically symmetric around each site and zero in the interstitial region. One could wonder whether we should use a spin-dependent spin-orbit potential  $\xi_i^s(r_i)$ , since this parameter is calculated from the potential  $V^s(r_i)$ , which is spin dependent. A full answer to this question is difficult since spin-orbit coupling is deduced from a relativistic Hamiltonian which is not spin dependent. For the present purpose, the eventual spin dependence of the spin-orbit parameter is a higher-order effect that can be neglected safely.<sup>42</sup>

Within the scattering formalism, perturbations are taken into account by expanding the Lippmann-Schwinger equation. Let  $f^\uparrow = f^{\uparrow\uparrow}(\mathbf{r})|\uparrow\rangle + f^{\uparrow\downarrow}(\mathbf{r})|\downarrow\rangle$  be the perturbed state corresponding to the unperturbed state  $\psi^\uparrow(\mathbf{r})|\uparrow\rangle$ . The Lippmann-Schwinger equation is written (with an implicit sum over sites)

$$\begin{pmatrix} f^{\uparrow\uparrow} \\ f^{\uparrow\downarrow} \end{pmatrix} = \begin{pmatrix} \psi^\uparrow \\ 0 \end{pmatrix} + \begin{pmatrix} G^+ & 0 \\ 0 & G^- \end{pmatrix} \xi(r) \begin{pmatrix} l^z & l^- \\ l^+ & -l^z \end{pmatrix} \begin{pmatrix} f^{\uparrow\uparrow} \\ f^{\uparrow\downarrow} \end{pmatrix}, \quad (44)$$

where  $l^\pm = l^x \pm il^y$ . Since the perturbation is small, we replace the perturbed state in the right-hand side by the un-

perturbed state, and we obtain the first Born approximation:

$$f^{\uparrow\uparrow}(\mathbf{r}_i) = \psi^\uparrow(\mathbf{r}_i) + \sum_j \int d^3r_j G^\uparrow(\mathbf{r}_i, \mathbf{r}_j) \xi_j(r_j) l_j^z \psi^\uparrow(\mathbf{r}_j), \quad (45)$$

$$f^{\uparrow\downarrow}(\mathbf{r}_i) = \sum_j \int d^3r_j G^\downarrow(\mathbf{r}_i, \mathbf{r}_j) \xi_j(r_j) l_j^+ \psi^\uparrow(\mathbf{r}_j). \quad (46)$$

Doing the same for the unperturbed state  $\psi^\downarrow$  gives

$$f^{\downarrow\uparrow}(\mathbf{r}_i) = \sum_j \int d^3r_j G^\uparrow(\mathbf{r}_i, \mathbf{r}_j) \xi_j(r_j) l_j^- \psi^\downarrow(\mathbf{r}_j), \quad (47)$$

$$f^{\downarrow\downarrow}(\mathbf{r}_i) = \psi^\downarrow(\mathbf{r}_i) - \sum_j \int d^3r_j G^\downarrow(\mathbf{r}_i, \mathbf{r}_j) \xi_j(r_j) l_j^z \psi^\downarrow(\mathbf{r}_j). \quad (48)$$

These equations mean that, when you send a pure up-spin state  $\psi^\uparrow(\mathbf{r}_i)$  in the crystal, the spin-orbit coupling at each site sends back a component without spin flip  $f^{\uparrow\uparrow}(\mathbf{r}_i)$  and a component where the initial spin up was flipped  $f^{\uparrow\downarrow}(\mathbf{r}_i)$ . The components with spin flip do not contribute to first order, and MXD comes from the fact that the action of spin-orbit coupling is reversed for a spin up and for a spin down.

The different unperturbed final states of a given energy are indexed by  $L_0$ . A sum over  $L_0$  amounts to the sum over final states in the absorption cross section (10). According to Ref. 43, the unperturbed state within the potential sphere of site  $j$  can be written

$$\psi_{L_0}^s(\mathbf{r}_j) = - \sum_\Lambda B_{j\Lambda}^s(L_0) R_{j\Lambda}^s(r_j) Y_\Lambda(\hat{\mathbf{r}}_j), \quad (49)$$

where the amplitudes  $B_{j\Lambda}^s(L_0)$  can be expressed in terms of the scattering path operators as

$$B_{j\Lambda}^s(L_0) = \kappa^s \sum_{i,L'} \tau_{j\Lambda i L'}^s J_{i L' L_0}^s. \quad (50)$$

The matrix  $J_{i L' L_0}^s$  is defined in Ref. 43 but will not be used in the final results. For the present work, it is sufficient to consider  $R_{j\Lambda}^s(r_j)$  as restricted to the muffin-tin sphere  $j$ .

Using the expression (8) for the Green function, we can write the Lippmann-Schwinger equation to first order around the photoabsorbing site  $i=0$ . In terms of these perturbed final states, the absorption cross section is<sup>43</sup>

$$\sigma(\hat{\mathbf{e}}) = 4\pi\alpha\hbar\omega(2m/\hbar^2) \sum_{L_0, m_j} (\kappa^\uparrow |\langle f_{L_0}^\uparrow | \hat{\mathbf{e}} \cdot \mathbf{r} | j m_j \rangle|^2 + \kappa^\downarrow |\langle f_{L_0}^\downarrow | \hat{\mathbf{e}} \cdot \mathbf{r} | j m_j \rangle|^2) \delta(E_f - E_i - \hbar\omega). \quad (51)$$

This formula could be used to calculate the influence of spin-orbit coupling in the final state of any edge, but we shall limit ourselves to the  $K$  edge. In that case, and keeping only the terms up to first order in the spin-orbit coupling we find the absorption cross section for left- and right-circular polarization:

$$\begin{aligned}
\sigma^\pm = 4\pi\alpha\hbar\omega(2m/\hbar^2)(1/3) & \left[ \kappa^\dagger M_{01}^{12} \sum_{L_0} |B_{01\pm 1}^\dagger(L_0)|^2 + \kappa^\downarrow M_{01}^{12} \sum_{L_0} |B_{01\pm 1}^\downarrow(L_0)|^2 \right. \\
& \pm 2\kappa^{12} M_{01}^\dagger M_{01}^{Z\dagger\dagger} \sum_{L_0} |B_{01\pm 1}^\dagger(L_0)|^2 \mp 2\kappa^{12} M_{01}^\downarrow M_{01}^{Z\downarrow\downarrow} \sum_{L_0} |B_{01\pm 1}^\downarrow(L_0)|^2 \\
& + 2\kappa^{13} M_{01}^{12} \sum_{jLL_0} \xi_{jl}^{\dagger\dagger} m \operatorname{Re}\{[B_{jL}^\dagger(L_0)]^* B_{01\pm 1}^\dagger(L_0)(\tau_{01\pm 1jL}^\dagger)^*\} \\
& \left. - 2\kappa^{13} M_{01}^{12} \sum_{jLL_0} \xi_{jl}^{\downarrow\downarrow} m \operatorname{Re}\{[B_{jL}^\downarrow(L_0)]^* B_{01\pm 1}^\downarrow(L_0)(\tau_{01\pm 1jL}^\downarrow)^*\} \right]. \quad (52)
\end{aligned}$$

Reduced matrix elements of the spin-orbit operator have been defined as

$$\xi_{jl}^{ss'} = \int_0^{\rho_j} dr_j r_j^2 R_{jl}^s(r_j) \xi_j(r_j) R_{jl}^{s'}(r_j), \quad (53)$$

$$Z_l^{ss'}(r) = \int_0^{\rho_0} dr' r'^2 R_{0l}^s(r^<) J_{0l}^s(r^>) \xi_0(r') R_{0l}^{s'}(r'), \quad (54)$$

where  $\rho_j$  is the muffin-tin radius of atomic sphere  $j$ ,  $J_{0l}^s(r)$  is the same as in Eq. (8). We have also defined atomic matrix elements:

$$M_{01}^s = \int_0^{\rho_0} dr r^3 R_{01}^s(r) \phi_{01/2}(r), \quad (55)$$

$$M_{01}^{Zss} = \int_0^{\rho_0} dr r^3 Z_1^{ss}(r) \phi_{01/2}(r). \quad (56)$$

$M_{01}^s$  is the atomic  $K$ -edge dipole transition amplitude,  $M_{01}^{Zss}$  is an atomic contribution to the effect of spin polarization on x-ray-absorption spectra.

## B. Green-function interpretation

Before discussing the physical meaning of expression (52), we shall rewrite it in terms of the scattering path operators. The optical theorem for scattering path operators is<sup>43</sup>

$$\sum_{L_0} [B_{jL}^s(L_0)]^* B_{01p}^s(L_0) = \frac{i\kappa^s}{2} [\tau_{01pjL}^s - (\tau_{jL01p}^s)^*]. \quad (57)$$

For the first four terms of expression (52), this gives us

$$\sum_{L_0} [B_{01p}^s(L_0)]^* B_{01p}^s(L_0) = -\kappa^s \operatorname{Im}(\tau_{01p01p}^s). \quad (58)$$

Since we study powdered samples, we must take the spherical average of (58), which is (see Ref. 36)

$$\left\langle \sum_{L_0} [B_{01p}^s(L_0)]^* B_{01p}^s(L_0) \right\rangle_\Omega = -\frac{\kappa^s}{\sqrt{3}} \operatorname{Im}(\tau_{00}^s(11;00)). \quad (59)$$

Notice that the sum does not depend on the polarization of the incident beam. The last two terms of Eq. (52) are

more delicate to evaluate. First we introduce Eq. (57) to obtain

$$\begin{aligned}
2 \sum_{L_0} \operatorname{Re}\{[B_{jL}^s(L_0)]^* B_{01p}^s(L_0)(\tau_{01pjL}^s)^*\} \\
= -\kappa^s \operatorname{Im}(\tau_{01pjL}^s \tau_{jL01p}^s). \quad (60)
\end{aligned}$$

Since we consider absorption by a powder, we must take the spherical average of the last two terms of Eq. (52). A lengthy but straightforward calculation yields

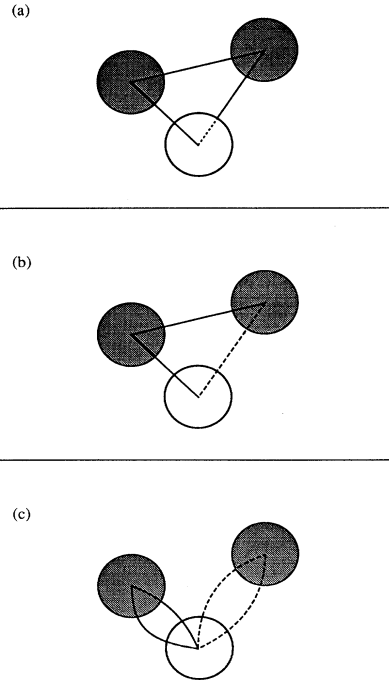


FIG. 2. The different ways spin-orbit coupling generates MXD at  $K$  edges. The action of spin-orbit coupling is a modification of the spatial part of the photoelectron state which depends on the photoelectron spin direction. The photoabsorbing atom is white, the neighbors are gray (see text).

$$\left\langle \sum_m m \tau_{01p'jL}^s \tau_{jL01p}^s \right\rangle = -\frac{p}{12} \delta_{p,p'} (-1)^l \sum_{a=|l-1|}^{a=l+1} [(l-a)(l+a+1)+2] \sum_{\alpha} (-1)^a {}^{-\alpha} \tau_{0j}^s(1l;a\alpha) \tau_{0j}^s(1l;a-\alpha). \quad (61)$$

Gathering all the above results, the absorption cross-section for left- and right-circularly polarized x rays, Eq. (52), takes the final form

$$\begin{aligned} \sigma^{\pm} = & -4\pi\alpha\hbar\omega(2m/\hbar^2)(1/3) \left[ \kappa^{\uparrow 2} M_{01}^{\uparrow 2} \frac{\text{Im}[\tau_{00}^{\uparrow}(11;00)]}{\sqrt{3}} + \kappa^{\downarrow 2} M_{01}^{\downarrow 2} \frac{\text{Im}[\tau_{00}^{\downarrow}(11;00)]}{\sqrt{3}} \right. \\ & \pm 2\kappa^{\uparrow 3} M_{01}^{\uparrow} M_{01}^{Z\uparrow\uparrow} \frac{\text{Im}[\tau_{00}^{\uparrow}(11;00)]}{\sqrt{3}} \mp 2\kappa^{\downarrow 3} M_{01}^{\downarrow} M_{01}^{Z\downarrow\downarrow} \frac{\text{Im}[\tau_{00}^{\downarrow}(11;00)]}{\sqrt{3}} \\ & \pm \kappa^{\uparrow 4} M_{01}^{\uparrow 2} \sum_{l,j} \frac{(-1)^l}{12} \zeta_{jl}^{\uparrow\uparrow} \sum_{a=|l-1|}^{a=l+1} [(l-a)(l+a+1)+2] \\ & \quad \times \sum_{\alpha} (-1)^{-\alpha} \text{Im}[\tau_{0j}^{\uparrow}(1l;a\alpha) \tau_{j0}^{\uparrow}(1l;a-\alpha)] \\ & \mp \kappa^{\downarrow 4} M_{01}^{\downarrow 2} \sum_{l,j} \frac{(-1)^l}{12} \zeta_{jl}^{\downarrow\downarrow} \sum_{a=|l-1|}^{a=l+1} [(l-a)(l+a+1)+2] \\ & \quad \left. \times \sum_{\alpha} (-1)^{-\alpha} \text{Im}[\tau_{0j}^{\downarrow}(1l;a\alpha) \tau_{j0}^{\downarrow}(1l;a-\alpha)] \right]. \quad (62) \end{aligned}$$

As for  $L_{\text{II,III}}$  edges, if the incident x-ray beam is only partially polarized and if the spin-quantization axis is not along the x-ray beam, then replace  $\pm$  by  $-P \cos\theta \sin 2\chi$  in Eq. (62).

The physical interpretation of the terms is now clearer. The first two terms represent the absorption cross section without taking into account spin-orbit coupling in the final state. As already stated, they do not present any dependence on the sense of circular polarization. The third and fourth terms are dichroic contributions where the up and down channels are separated by spin-orbit coupling on the photoabsorbing site. The fifth and sixth terms are dichroic contributions where the up and down channels are separated by spin-orbit coupling on all the sites (including the photoabsorbing site). An image of the last two terms would be as follows: the  $|1p\rangle$  wave of the photoelectron ejected by absorption of a  $p = \pm 1$  circular x ray is transported to the site  $j$  by the scattering path operator  $\tau_{0j}$ . At site  $j$  the  $|lm\rangle$  component of the photoelectron wave function is scattered by the spin-orbit potential. This scattering depends on the sign of  $m$ , which itself depends on the sign of  $p$ . Then the modified wave is transported back to the absorbing site by the scattering path operator  $\tau_{j0}$ . The third and fourth terms come from the second (atomiclike) term of the Green function (8) while the fifth and sixth terms come from the first term of the Green function which corresponds to specific properties of the crystal. This is the reason why scattering path operators appear twice in the fifth and sixth terms. A pictorial representation of the various contributions to MXD at  $K$  edges is summarized in Fig. 2 (which should not be taken too literally). Processes (a) corresponds to the third and fourth terms of Eq. (62), processes (b) and (c) correspond to the fifth and sixth terms.

The difference between MXD at  $K$  edges and at  $L_{\text{II,III}}$  edges is apparent. In the latter case, the effect is related to the spin-up and spin-down states through coefficients

which depend neither on energy nor on atomic species. The analysis of  $K$ -edge MXD spectra is much more delicate, because the coefficients weighting the spin-up and spin-down states ( $M_{01}^s M_{01}^{Zss}$  and  $\zeta_{jl}^{ss}$ ) depend on energy, on the photoabsorbing species, and on the neighbor atom species.

### C. Evaluation of atomic matrix elements

We give now the results of approximate calculations carried out for  $K$ -edge spectra of iron. We also made calculations for cobalt and nickel, but since the results are qualitatively similar, we show only the case of iron. Figure 3 shows the electric-dipole transition probabilities  $M_{01}^{\uparrow 2}$  and  $M_{01}^{\downarrow 2}$  from the  $1s$  core hole to the spin-polarized

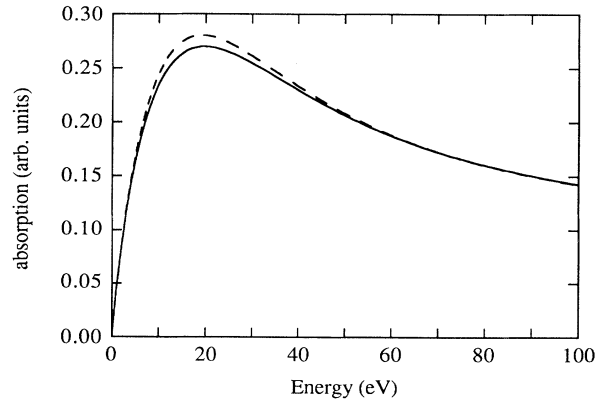


FIG. 3. Electric-dipole atomic transition probabilities for iron [first two terms of Eq. (62)]. Dashed line,  $M_{01}^{\uparrow 2}$ ; solid line,  $M_{01}^{\downarrow 2}$ . Up spins are majority spins.

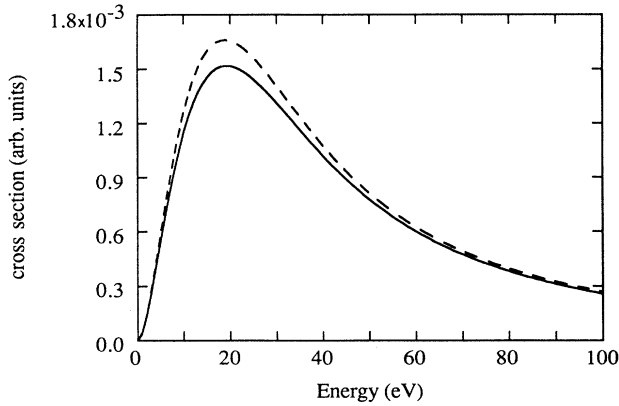


FIG. 4. Atomic spin-orbit matrix element of the first kind for iron [third and fourth terms of Eq. (62), i.e., process (a) of Fig. 2]. Dashed line,  $M_{01}^1 M_{01}^{21}$ ; solid line,  $M_{01}^1 M_{01}^{11}$ . Units are arbitrary but consistent with those of Fig. 3.

$p$  states of iron. There is a noticeable difference for the transitions towards up and down spins; however, this difference cannot be reached experimentally as in the case of  $L_{II,III}$ -edge spectra, because there is no spin-orbit coupling in the initial state. The terms that cause the MXD effect at  $K$  edges are shown in Figs. 4 and 5.

The atomic contributions to the third and fourth terms of Eq. (62) are drawn in Fig. 4. These terms correspond to process (a) of Fig. 2. The atomic contributions to the fifth and sixth terms of Eq. (62) for the central atom ( $j=0$ ) and  $l=1$  are drawn in Fig. 5. These terms correspond to process (c) of Fig. 2. It was shown by Parlebas<sup>44</sup> that nondiagonal Green functions are generally smaller than diagonal ones. In terms of scattering path operators, this means that  $\tau_{00}$  is generally larger than  $\tau_{0j}$ . A

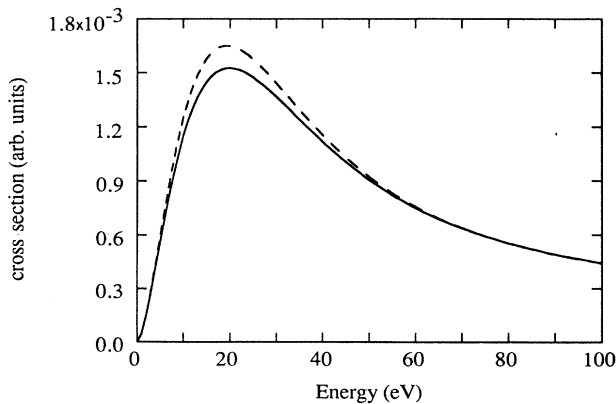


FIG. 5. Atomic spin-orbit matrix element of the second kind for iron [fifth and sixth terms of Eq. (62) for central atom, i.e., process (c) of Fig. 2] for  $l=1$ . Dashed line,  $M_{01}^{12} \xi_{01}^{11}$ ; solid line,  $M_{01}^{12} \xi_{01}^{11}$ . Units are arbitrary but consistent with those of Fig. 3.

multiple-scattering expansion of  $\tau_{00}$  and  $\tau_{0j}$  up to second order confirms that the intra-atomic terms ( $j=0$ ) are dominant. Therefore Figs. 4 and 5 represent the main contributions to the MXD effect at  $K$  edges. Comparison with Fig. 3 shows that their order of magnitude is 0.5%, which is consistent with experiment.<sup>6-8</sup>

We noticed that SPEXAFS was weak at  $K$  edges of transition metals. This can be understood by looking at Figs. 4 and 5 which show weighting factors of the fine structure. Contrary to the case of  $L_{II,III}$ -edge spectra where these coefficients are constant, the  $K$ -edge weighting factors decrease with energy and tend to zero at high energy. At 100 eV, SPEXAFS oscillations are already decreased by a factor of 5.

## V. CONNECTION TO BAND-STRUCTURE FORMALISM

The theoretical studies of magnetic materials are usually made within the band-structure formalism. In this section, we shall use the equivalence between multiple-scattering and band-structure calculations<sup>45</sup> to give an interpretation of our results in terms of density of spin-up and spin-down states, which is more familiar. Up to now, all published comparisons of  $M \times D$  spectra with band-structure calculations have neglected the effect of the core hole on spin density of states. If this effect is important, the multiple-scattering formalism or more sophisticated band-structure methods<sup>46</sup> should be used.

The formal manipulations we shall use in this section are drawn from Ref. 47. In band-structure theory, the final states are indexed according to the Bloch vector  $\mathbf{k}$  and the band index  $n$ . Therefore the absorption cross section (11) becomes

$$\sigma(\hat{\mathbf{e}}, \omega) = 4\pi^2 \alpha \hbar \omega \sum_{\mathbf{k}, n, m_j} (|\langle f_{\mathbf{k}n}^\uparrow | \hat{\mathbf{e}} \cdot \mathbf{r} | j m_j \rangle|^2 + |\langle f_{\mathbf{k}n}^\downarrow | \hat{\mathbf{e}} \cdot \mathbf{r} | j m_j \rangle|^2) \times \delta(E_{\mathbf{k}n}^s - E_i - \hbar\omega). \quad (63)$$

We can expand the final-state wave function  $f_{\mathbf{k}n}^s$  corresponding to the energy  $E_{\mathbf{k}n}^s = E_i + \hbar\omega$  over spherical harmonics

$$f_{\mathbf{k}n}^s(\mathbf{r}) = \sum_L f_{\mathbf{k}n}^s(r, L) Y_L(\hat{\mathbf{r}}). \quad (64)$$

Inside each atomic sphere, the potential is spherical, so that  $f_{\mathbf{k}n}^s(r, L)$  is a regular solution of the radial Schrödinger equation (9). All regular solutions of the Schrödinger equation (9) are proportional. Thus there exist constants  $\alpha_{\mathbf{k}n}^s(L)$  such as

$$f_{\mathbf{k}n}^s(r, L) = \alpha_{\mathbf{k}n}^s(L) R_{0l}^s(r), \quad (65)$$

where  $R_{0l}^s(r)$  is the absorbing atom radial wave function for energy  $E = E_i + \hbar\omega$  defined in Sec. II.

With these notations, we can repeat the calculation of Sec. III and we obtain, for  $L_{II,III}$  edges, equations identical to (25)–(28) with the new definition:

$$\sigma_{ij}^s = 4\pi^2 \alpha \hbar \omega \frac{1}{9(2l+1)} (M_{ij}^s)^2 N_i^s(E), \quad (66)$$

where  $N_j^s(E)$  is an  $l$ -projected density of states around the photoabsorbing site, defined as

$$N_j^s(E) = \sum_{k,n,m} |\alpha_{kn}^s(l,m)|^2 \delta(E_{kn}^s - E). \quad (67)$$

Equation (66) is the basic formula used to analyze most magnetic x-ray dichroism spectra obtained up to now. It is similar to the expression derived by Schütz *et al.*<sup>6,7,10,11,13</sup> Since the atomic factor  $M_{ij}^s$  is smooth, information concerning the spin polarization of the  $l$ -projected density of states can be obtained from MXD spectra. For example, when measuring MXD spectra at the  $L_{II,III}$  edges of rare earths, one probes the spin polarization of the  $d$  states of the absorbing rare-earth atom. MXD is thus a unique tool to investigate magnetic contributions, since it is selective in atomic species and in orbital symmetry. The same kind of analysis is not rigorously valid for  $K$ -edge MXD spectra, as seen in Sec. IV. However, an investigation of the spin polarization of  $p$  orbitals may be possible, using carefully chosen reference compounds. Furthermore, calculated spin-orbit matrix elements can be helpful. For instance, we saw in Sec. IV C that these matrix elements are positive for iron. Therefore a discussion analogous to that of Sec. III B shows that, when the MXD signal is positive, a majority of spins are down (with the provisos made at the end of Sec. IV B). This leads to the well-known conclusion that  $4p$  spins are coupled ferromagnetically to  $3d$  spins in iron.

In Eq. (66), the atomic transition probability  $M_{ij}^s$  can be calculated from atomic potentials, and does not depend strongly on the position and nature of the neighboring atoms. The spin-polarized projected density of states  $N_j^s(E)$  can be obtained from *ab initio* or tight-binding calculations. Therefore it is possible to take advantage of band-structure calculations to interpret experimental spectra, as was done in Ref. 7.

## VI. CONCLUSION

We have tried to give an account of magnetic x-ray circular dichroism in itinerant magnetic materials that synthesizes the heuristic qualities of the model developed by Schütz *et al.* and the quantitative approach of the theory presented by Strange and collaborators.

According to the present work, MXD is due to an interplay between spin-orbit interaction and magnetic spin polarization. At  $L_{II,III}$  edges, a large spin-orbit coupling exists in the initial state, and MXD spectra supply information concerning the spin polarization of the unoccupied  $d$  states. The driving mechanism for this is the mixing of spin and space variables in the initial state that implies preferential electric-dipole transitions towards

definite spin states (see Fig. 1). For the example of an  $L_{II}$  edge obtained with left-circular x rays, the strong dipole transition  $|j = \frac{1}{2}, m_j = \frac{1}{2}\rangle \rightarrow |l = 2, m = 2, m_s = -\frac{1}{2}\rangle$  implies that, at an  $L_{II}$  edge, left-circular x rays make preferential transitions towards down-spin states. This allows for an experimental determination of the spin orientation of the  $d$  orbitals of a given atomic species in the sample relative to the external magnetic field direction. Thus MXD spectra yield very simply the coupling (ferromagnetic or antiferromagnetic) of the spins of the  $d$  orbitals of each atomic species relative to the total magnetic moment. Together with magnetic diffraction studies, this allows for the determination of the spin and orbital contributions to magnetism. Moreover, by using our formula describing the spin-polarized extended x-ray-absorption fine structure, it is possible to investigate the spin polarization of the photoabsorbing atom and of its neighbors. In that case, we switch from a density-of-states approach to the multiple-scattering theory which describes the spin polarization of each atomic potential in the sample.

The case of MXD at  $K$  edges is more involved because spin-orbit coupling interacts directly with the photoelectron.

In Sec. V, we have described how band-structure results can be used within our multiple-scattering approach. This makes clearer the validity of the usual analysis of experimental results, where MXD spectra are directly compared with spin-polarized density of states.

The purpose of the present paper was to study the physical principles underlying magnetic x-ray circular dichroism. Practical calculations of MXD spectra are based on the local spin-density approximation (LSDA). However, the range of validity of the Green-function approach we used in this paper is broader than that of LSDA, since it is a consequence of optical potential theory.<sup>48,49</sup> Therefore the physical principles we emphasized may be correct even when the LSDA breaks down.

## ACKNOWLEDGMENTS

This paper was undertaken on the advice of Professor G. Krill, Dr. J. Goulon, and Professor F. Gautier. The physical understanding of the formulas was thoroughly discussed with Professor G. Krill, Professor M. Piecuch, Professor E. Dartyge and Professor F. Gautier. The description of the band-structure approach has greatly benefited from Dr. Czyżyk's advice. Let them all be warmly thanked. Last but not least, one of us (C.B.) wants to acknowledge his debt to Professor C. R. Natoli, who taught him the multiple-scattering concepts required to carry out this calculation.

<sup>1</sup>A. H. Forman, Phys. Rev. **3**, 306 (1914); **7**, 119 (1916).

<sup>2</sup>G. van der Laan, B. T. Thole, G. A. Sawatzky, J. B. Goedkoop, J. C. Fuggle, J.-M. Esteve, R. C. Karnatak, J. P. Remeika, and H. A. Dabkowska, Phys. Rev. B **34**, 6529 (1986).

<sup>3</sup>J. Bonarski and J. Karp, J. Phys. Condens. Matter **1**, 9261 (1989).

<sup>4</sup>D. P. Siddons, M. Hart, Y. Amemiya, and J. B. Hastings, Phys. Rev. Lett. **64**, 1967 (1990).

<sup>5</sup>J. B. Goedkoop, J. C. Fuggle, B. T. Thole, G. van der Laan, and G. A. Sawatzky, Nucl. Instrum. Methods A **273**, 429 (1988).

<sup>6</sup>G. Schütz, W. Wagner, W. Wilhelm, P. Kienle, R. Zeller, R.

- Frahm, and G. Materlik, *Phys. Rev. Lett.* **58**, 737 (1987).
- <sup>7</sup>G. Schütz and R. Wienke, *Hyperfine Interactions* **50**, 457 (1989).
- <sup>8</sup>S. P. Collins, M. J. Cooper, A. Brahmia, D. Laundry, and T. Pitkanens, *J. Phys. Condens. Matter* **1**, 323 (1989).
- <sup>9</sup>C. T. Chen, F. Sette, Y. Ma, and S. Modesti, *Phys. Rev. B* **42**, 7262 (1990).
- <sup>10</sup>M. Knülle, Ph.D. thesis, University of Munich, 1988.
- <sup>11</sup>G. Schütz, M. Knülle, R. Wienke, W. Wilhelm, W. Wagner, P. Kienle, and R. Frahm, *Z. Phys. B: Condens. Matter* **73**, 67 (1988).
- <sup>12</sup>G. Schütz, R. Frahm, P. Mautner, R. Wienke, W. Wagner, W. Wilhelm, and P. Kienle, *Phys. Rev. Lett.* **62**, 2620 (1989).
- <sup>13</sup>G. Schütz, R. Wienke, W. Wilhelm, W. Wagner, P. Kienle, R. Zeller, and R. Frahm, *Z. Phys. B: Condens. Matter* **75**, 495 (1989).
- <sup>14</sup>J. B. Goedkoop, Ph.D. thesis, University of Nijmegen, The Netherlands, 1989.
- <sup>15</sup>F. Baudelet, E. Dartyge, G. Krill, J.-P. Kappler, C. Brouder, M. Piecuch, and A. Fontaine, *Europhys. Lett.* (to be published).
- <sup>16</sup>F. Baudelet, E. Dartyge, G. Krill, J.-P. Kappler, C. Brouder, M. Piecuch, and A. Fontaine, *Phys. Rev. B* **43**, 3809 (1991).
- <sup>17</sup>B. T. Thole, G. van der Laan, and G. A. Sawatzky, *Phys. Rev. Lett.* **55**, 2086 (1985).
- <sup>18</sup>J. B. Goedkoop, B. T. Thole, G. van der Laan, G. A. Sawatzky, F. M. F. de Groot, and J. C. Fuggle, *Phys. Rev. B* **37**, 2086 (1988).
- <sup>19</sup>J. L. Erskine and E. A. Stern, *Phys. Rev. B* **12**, 5016 (1975).
- <sup>20</sup>P. Strange, H. Ebert, J. B. Staunton, and B. L. Gyorffy, *J. Phys. Condens. Matter* **1**, 2959 (1989).
- <sup>21</sup>H. Ebert, B. Drittler, R. Zeller, and G. Schütz, *Solid State Commun.* **69**, 485 (1989).
- <sup>22</sup>H. Ebert, P. Strange, and B. L. Gyorffy, *J. Appl. Phys.* **63**, 3055 (1988).
- <sup>23</sup>H. Ebert and R. Zeller, *Physica B+C* **161B**, 191 (1989).
- <sup>24</sup>H. Ebert, P. Strange, and B. L. Gyorffy, *J. Phys. (Paris) Colloq.* **49**, C8-31 (1988).
- <sup>25</sup>H. Ebert, P. Strange, and B. L. Gyorffy, *Z. Phys. B* **73**, 77 (1988).
- <sup>26</sup>C. Brouder, *J. Phys. Condens. Matter* **2**, 701 (1990).
- <sup>27</sup>P. Carra and M. Altarelli, *Phys. Rev. Lett.* **64**, 1286 (1990).
- <sup>28</sup>C. Brouder, D. Malterre, and G. Krill, in *Proceedings of the Spring School Rayonnement Synchrotron Polarisé, Electrons Polarisés et Magnétisme, Mittelwihr, France, 1989*, edited by E. Beaurepaire, B. Carriere, and J.-P. Kappler (University of Strasbourg, Strasbourg, 1990), p. 115.
- <sup>29</sup>P. Bruno, *Phys. Rev. B* **39**, 865 (1989).
- <sup>30</sup>O. Gunnarsson, *J. Phys. F* **6**, 587 (1976); R. O. Jones and O. Gunnarsson, *Rev. Mod. Phys.* **61**, 689 (1989).
- <sup>31</sup>M. Benfatto, in *Proceedings of Progress in X-Ray Synchrotron Radiation Research, 2nd European Conference, Rome, Italy, 1989*, edited by A. Balerna, E. Bernieri and S. Mobilio (Italian Physical Society, Bologna, in press), p. 3.
- <sup>32</sup>P. J. Durham, in *X-Ray Absorption*, edited by D. C. Koningsberger and R. Prins (Wiley, New York, 1988), p. 67.
- <sup>33</sup>R. Feder, in *Polarized Electrons in Surface Physics* (World Scientific, Singapore, 1985), p. 125.
- <sup>34</sup>M. Born and E. Wolf, *Principles of Optics*, 6th ed. (Pergamon, Oxford, 1980).
- <sup>35</sup>L. C. Biedenharn and J. D. Louck, *Angular Momentum in Quantum Physics*, Vol. 8 of *Encyclopedia of Mathematics* (Addison-Wesley, Reading, MA, 1981).
- <sup>36</sup>C. Brouder, M. F. Ruiz-López, R. F. Pettifer, C. R. Natoli, and M. Benfatto, *Phys. Rev. B* **39**, 1488 (1989).
- <sup>37</sup>B. K. Teo and P. A. Lee, *J. Am. Chem. Soc.* **101**, 2815 (1979).
- <sup>38</sup>*Handbook of Mathematical Functions*, edited by M. Abramowitz and I. A. Stegun (Dover, New York, 1965).
- <sup>39</sup>V. L. Moruzzi, J. F. Janak, and A. R. Williams, *Calculated Electronic Properties of Metals* (Pergamon, New York, 1978).
- <sup>40</sup>V. A. Belyakov and V. E. Dmitrienko, *Usp. Fiz. Nauk.* **158**, 679 (1989) [*Sov. Phys.—Usp.* **32**, 697 (1989)].
- <sup>41</sup>J. Friedel, P. Lengart, and G. Leman, *J. Phys. Chem. Solids* **25**, 781 (1964).
- <sup>42</sup>G. H. O. Daalderop, P. J. Kelly, and M. F. H. Schuurmans, *Phys. Rev. B* **41**, 11 919 (1990).
- <sup>43</sup>C. R. Natoli, M. Benfatto, and S. Doniach, *Phys. Rev. B* **34**, 4682 (1986).
- <sup>44</sup>J. C. Parlebas, Ph.D. thesis, University of Strasbourg, 1974.
- <sup>45</sup>C. R. Natoli and M. Benfatto, *J. Phys. (Paris) Colloq.* **47**, C8-11 (1986).
- <sup>46</sup>P. J. W. Weijs, M. T. Czyżyk, J. F. van Acker, W. Speier, J. B. Goedkoop, H. van Leuken, H. J. M. Hendrix, R. A. de Groot, G. van der Laan, K. H. J. Buschow, G. Wiech, and J. C. Fuggle, *Phys. Rev. B* **41**, 11 899 (1990); M. T. Czyżyk and R. A. de Groot, in Ref. 31, p. 47.
- <sup>47</sup>J. E. Müller and J. W. Wilkins, *Phys. Rev. B* **29**, 4331 (1984).
- <sup>48</sup>H.-D. Meyer, *Phys. Rev. A* **40**, 5605 (1989).
- <sup>49</sup>A. Jain, C. A. Weatherford, D. G. Thompson, and P. McNaughten, *Phys. Rev. A* **40**, 6730 (1989).